0013-7227/00/$03.00/0
Endocrinology

Vol. 141, No. 8
Printed in U.S.A.

The 3′-Untranslated Region of the Human Estrogen Receptor α Gene Mediates Rapid Messenger Ribonucleic Acid Turnover*

MARY-ROSE KENEALY, GILLES FLOURIOT, VERA SONNTAG-BUCK, THOMAS DANDEKAR, HEIKE BRAND, AND FRANK GANNON

Department of Microbiology, National University of Ireland (M.R.K.), Galway, Ireland; and European Molecular Biology Laboratory (G.F., V.S.B., T.D., H.B., F.G.), 69012 Heidelberg, Germany

ABSTRACT

Human estrogen receptor-α messenger RNA (hERα mRNA) has a relatively short half-life, which was determined to be approximately 5 h in MCF-7 cell line after actinomycin D treatment. The 3′-untranslated region (3′UTR) of hERα mRNA was previously shown to completely down-regulate chloramphenicol acetyltransferase activity when present at the 3′-end of chloramphenicol acetyltransferase transcripts, suggesting a destabilizing function of the hERα 3′UTR sequence. Chimeric genes composed of a serum-inducible Fos promoter, GH-coding sequences, and different segments of the hERα complementary DNA 3′UTR sequence were used to confirm this hypothesis and to localize the RNA region responsible for the destabilizing effect. The presence of the complete hERα 3′UTR reduced the half-life of the reporter mRNA from more than 24 to 3 h. When the hERα 3′UTR was subdivided into four fragments (UTR1–4), one fragment, UTR2, retained the most ability to down-regulate the reporter mRNA ($t_{1/2}$ = 4 h). A stretch of four AUUUA motifs within UTR2 was shown not to mediate mRNA destabilization. In contrast, further subdivision of the UTR2 into three parts (UTR2a–c) resulted in the loss of the destabilizing activity. Finally, recombination of two UTR2 subfragments (UTR2a and -b) partially restored this function, indicating a cooperative role among the three UTR2a–c subfragments in the process that leads to destabilization of the hERα transcript. (*Endocrinology* **141:** 2805–2813, 2000)

ESTROGEN RECEPTOR α (ERα) plays a key role in many normal physiological processes, ranging from female sexual development and reproduction to liver, fat, and bone cell metabolism (1–3). The ERα has been shown to be also involved in the biology of breast cancer and is used clinically as an important prognostic factor (4). Therefore, elucidation of the molecular mechanisms that control the expression of the ERα gene should provide crucial information concerning not only the differential tissue and temporal ERα expressions in estrogen target cells, but also its involvement in pathological processes. We recently extended earlier observations to show that the human ERα gene was a complex genomic unit exhibiting alternative splicing and promoter usage in a tissue-specific manner (5). This demonstrated the importance of transcriptional control in the regulation of ERα expression. Nevertheless, several other reports indicate that ERα mRNA stability is subject to hormonal control (6–9), suggesting that the regulation of ERα expression may occur also at a posttranscriptional level.

ERα is a member of the multigene nuclear receptor family, and an unusual feature of this family is the conservation of a very long 3′-untranslated region (3′UTR), which is usually 2 times as long as the coding region (10, 11). The human ERα 3′UTR is 4.3 kb in length (10). When the availability of the 3′UTR sequences of the different nuclear receptor genes allows comparisons to be made, there seems to be higher than expected sequence identity between species. Unfortunately, in addition to the human ERα 3′UTR, only 80 bp of rodent ERα 3′UTR (12, 13) are known, and thus there are no closely related species to search for conserved sequences within the mammalian ERα 3′UTRs. However, when the ER 3′UTR sequences of two avian species, chicken (P. Nestor, C. Murphy, and F. Gannon, unpublished data) and zebra finch (14), are compared with each other, there is 75% identity over 900 bp, and more complete comparisons between human and chicken ER 3′UTR sequences also show some regions of extensive identity. These observations prompted an investigation into the possible functional role for the ERα 3′UTR in posttranscriptional control of ERα expression.

Sequence analysis of the hERα 3′UTR indicated that this region is more AU rich than the coding region, as it contains long tracts of AU-rich sequence as well as 13 copies of AUUUA (10, 11). AU-rich elements (AREs) and AUUUA motifs have been shown in many cases to mediate mRNA destabilization. They were first identified as having functional roles in the very unstable mRNAs, *e.g.* protooncogenes c-*fos* (15) and c-*myc* (16), the cytokine granulocyte-macrophage colony-stimulating factor (17), and a number of genes that encode interleukins and interferons (18, 19), where rapid mRNA turnover is required for appropriate responses to control signals. Therefore, the possibility that ARE could have a role in directing hERα mRNA destabilization was suggested (11).

The destabilizing function of the hERα 3′UTR sequence is demonstrated in this report. The decay kinetics of chimeric transcripts, containing the hERα 3′UTR or shorter fragments

Received May 4, 2000.
Address all correspondence and requests for reprints to: Dr. Frank Gannon, EMBL, Postfach 10.2209, Meyerhofstrasse 1, D-69012, Heidelberg, Germany. E-mail: Gannon@EMBL-Heidelberg.de.
* This work was supported by grants from the Health Research Board of Ireland, the Irish Cancer Research Advancement Board, EMBO, and the Irish-American Partnership.

of it, were studied in a stably transformed cell culture in an attempt to delineate destabilizing regions. A 1-kb subfragment of the hERα 3′UTR still retained destabilizing activity. Surprisingly, a stretch of four AUUUA motifs within this fragment was not responsible for that destabilization. In contrast, a cooperative role between different regions of this 1-kb subfragment was shown to be required for a significant destabilizing effect.

Materials and Methods

Plasmid constructions

The plasmid pfGH used for the chimeric constructs in the stable transfection experiments was provided by G. Goodall (Institute of Medical and Veterinary Science, Adelaide, Australia) (20). To generate pfGH+hER 3′UTR, the 3.895-kb *Eco*RI/*Xho*I fragment containing hERα 3′UTR [from nucleotides (nt) 2369–6264] was digested from p3′hER2 (21) and subcloned first into PCR II cloning vector (Invitrogen, Leek, The Netherlands) previously digested with *Eco*RI and *Xho*I. A *Kpn*I/*Xho*I fragment, including the 3.895-kb ER 3′UTR sequence, was digested from that and ligated into the unique *Kpn*I/*Sac*I site in the bovine GH 3′UTR of the pfGH vector along with a 100-bp *Xho*I/*Sac*I fragment from Bluescript (Stratagene, La Jolla, CA) that acted as a bridging fragment. PCR was performed using the p3′hER plasmid or human genomic DNA as a template to generate four fragments spanning the entire hER 3′UTR (UTR1–4). The primers were designed to introduce a *Kpn*I or *Sac*I site to the 5′- and 3′-ends of the PCR products to facilitate subcloning into the *Kpn*I/*Sac*I site of the pfGH plasmid. The following 5′- and 3′-primers were used for the four constructs: 3′1k and 3′1s (2034–3397) for UTR1, 3′2k and 3′2s (3384–4464) for UTR2, 3′3k and 3′3s (4450–5497) for UTR3, and 3′4k and 3′4kk (5503–6305) for UTR4 (the numbers in *parentheses* refer to the hERα sequence as published in Ref. 10).

UTR2 was further subdivided into three PCR-generated fragments (UTR2a–c) using the following primer pairs: 3′2k and 2a3′ (3384–4030) for UTR2a, 2b5′ and 2b3′ (4031–4173) for UTR2b, and 2c5′ and 3′2s (4174–4464) for UTR2c. UTR2(AU)mut and UTR2b(AU)mut cover the same sequence as UTR2 and UTR2b, respectively, except that the four ATTTA motifs within them were mutated to ACCCA. This mutation in UTR2b(AU)mut was performed by changing the sequence in the long PCR primers used, 2d5′ and 2d3′, to generate the mutated PCR product. UTR2(AU)mut was amplified by PCR in 2 rounds of 30 cycles using the long primers UTR2b(AU)mut sense and antisense [sequences identical to UTR2b(AU)mut] with the primers 3′2k and 3′2s. The mutated sequences were confirmed by sequencing. Constructs containing the longer recombined PCR-generated subfragments were prepared using primer pairs 3′2k and 2b3′ for UTR2(a+b) (3384–4173) and 2b5′ and 3′2s for UTR2(b+c) (4031–4064). Again, a *Kpn*I or *Sac*I site was incorporated into all primers to enable subcloning directly into pfGH.

Templates used to prepare the double stranded probes labeled by random priming were obtained as follows. To detect hER mRNA from MCF-7 cells, a PCR product (exons 1–8) was amplified from hERα complementary DNA. For the control probe 36B4, a 220-bp *Pst*I fragment from a pBR322 plasmid containing the sequence for the constitutively expressed gene 36B4 (provided by P. Chambon, Institut de Génétique et de Biologie Moléculaire et Cellulaire, Centre National de la Recherche Scientifique/Institut National de la Santé et de la Recherche Médicale/Université Louis Pasteur, Illkirch, France) (22) was subcloned into Bluescript. PCR products were amplified with flanking vector primers and then used as a template for labeling. For the GH probe, a fragment from the GH-coding region of pfGH (681–1060) was amplified from that plasmid using the primers 5′GHcod and 3′GHcod.

Primers

The following primers were used: 3′1k, GGTACCCCCACACGGTTCAGATAATC; 3′1s, GAGCTCGGACCAGTCTAATGCATACG; 3′2k, GGTACCCAGATTACGTATGCCCC; 3′2s, GAGCTCGTATTACATCGTCTAGTC; 3′3k, GGTACCGACGATGTAATACCAG; 3′3s, GAGCTCTGCCTTTCACATAACTA; 3′4k, GGTACCGTTCATACAGTAGCTCAA; 3′4kk, GGTACCGAACATCAAATAGGTTGA; 2a3′, GTAGCACGAGCTCCAGAATTACTACATTCAATTG; 2b5′, TGATCGGGGTACCGGATTTAATTTGACTGGGTT; 2b3′, GTAGCACGAGCTCATTTAAATGAATAATCACC; 2c5′, TGATCGGGGTACCGAAGATCACATTTCATATCAAC; 2d5′, TGATCGGGGTACCGGACCCAATTTGACTGGGTTAACATGCAAAAACCAAGGAAAAATACCCAGTTTTTT; 2d3′, GTAGCACGAGCTCATTTGGGTGAATAATCACCAGGCTTTAGGCATGGGTGACTGTA; 5′GHcod, TGGCTTTTGGCCTGCTCT; and 3′GHcod, CATAGACGTTGCTGTCAG.

Cell culture and transfections

MCF-7 cell lines were maintained in DMEM with L-glutamine (BioWhittaker, Inc., Verviers, Belgium) supplemented with 10% FCS (BioWhittaker, Inc.), penicillin (50 IU/ml), and streptomycin (50 μg/ml; Life Technologies, Inc., Paisley, Scotland) at 37 C under 5% CO_2. To analyze the endogenous hERα mRNA decay rate in MCF-7 cells, actinomycin D (Sigma, Poole, UK) was added to the medium at a final concentration of 0.5 μg/ml, and cells were harvested for RNA isolation at various points from 0–24 h after actinomycin D treatment.

HeLa cells were maintained under the same conditions as described above. Stably transfected cell lines were prepared by transfecting 10 μg pfGH construct plasmids according to the calcium phosphate method (23). Forty-eight hours later cells were grown in 600 μg/ml G418 sulfate (Geneticin, Life Technologies, Inc.) to select for the neo marker that was included on the pfGH plasmid. Resistant colonies were pooled, and cell lines were maintained in 300 μg/ml G418 sulfate thereafter.

For the time-course experiments, cells grown to 50% confluence in 10% FCS in DMEM were washed twice with PBS and then cultivated for 48 h in 0.5% FCS-DMEM as a serum deprivation step. Then cells were stimulated by adding 20% FCS-DMEM to induce the c-*fos* promoter. Harvesting for RNA isolation was carried out at 0, 2, 4, 6, 9, 12, and 24 h after serum stimulation.

RNA preparation and analysis

Total RNA was isolated from harvested cells using the LiCl-urea method (24). Thirty-microgram aliquots of RNA were electrophoresed through 1.2% agarose gels in the presence of formaldehyde and transferred overnight to Hybond N membranes (Amersham International, Aylesbury, UK). After fixing the membranes by UV cross-linking, they were prehybridized at 42 C for 3–6 h in 50% formamide, 5 × SSC (standard saline citrate), 5 × Denhardt's solution, 0.5% SDS, and 100 μg/ml denatured salmon testis DNA. Hybridization was carried out at 42 C overnight in the same solution but also including 50 μg/ml salmon testis DNA and a final concentration of 1×10^6 cpm/ml ^{32}P-labeled probe. Double stranded probes (GH-coding region) were labeled using the random prime labeling kit, High Prime (Roche Molecular Biochemicals, Mannheim, Germany). After hybridization, blots were washed twice in 2 × SSC-0.1% SDS at room temperature for 10 min and then twice in 0.2 × SSC-0.1% SDS at 55 C for 45 min. Membranes were exposed to x-ray film (Eastman Kodak Co., Rochester, NY) at −70 C. To rehybridize with the 36B4 control probe the first probes were stripped from the membrane by immersing in freshly boiled 0.5% SDS solution and were allowed to cool to room temperature before hybridizing again, as described above.

Autoradiographs were scanned using a ScanMaker III (Microtek Electroniks GmBH, Dusseldorf, Germany) and ScanWizard (Polaroid, Cambridge, MA) and Adobe PhotoShop (Macintosh, San José, CA) software. Signals were quantified using the NIH Image 1.54 program. All signals were also quantified using the Vilber Lourmat detection system and Bioprint/Bio1d V.96 software (Vilber Lourmat, Torcy, France) to verify the densitometry results. Densitometric values for GH signals were normalized using the values obtained for the internal reference, 36B4.

Results

The endogenous hERα mRNA half-life in MCF-7 cells after actinomycin D treatment is 5 h

The breast carcinoma cell line MCF-7 expresses ERα mRNA at a relatively high level and is the most widely used in ERα expression studies. This cell line was chosen to study the endogenous ERα mRNA decay rate. Cells were grown in DMEM with normal FCS, as were all cell lines when analyzing decay rates of any transcript described in this paper.

MCF-7 cells were harvested at various time points after addition of the transcription inhibitor actinomycin D at 0.5 μg/ml to the medium. Northern blot analysis of the cellular RNA, performed using a probe spanning the coding region of ERα mRNA, is shown in Fig. 1A. Densitometric analysis of the ERα mRNA signal was normalized by measuring the 18S ribosomal mRNA band after methylene blue staining. The half-life of ERα mRNA was deduced to be approximately 5 h in the presence of actinomycin D (Fig. 1B).

hERα 3′UTR reduces the half-life of an otherwise stable reporter mRNA

Transient transfection experiments have previously shown that when the almost complete hERα 3′UTR (the 3.9-kb *Eco*RI/*Xho*I fragment) is cloned downstream of the chloramphenicol acetyltransferase (CAT)-coding region of the KSSV2 expression vector as part of the mRNA transcript, it caused a reduction to basal levels of CAT activity (11). The down-regulating activity was specific to the hERα 3′UTR, as the insertion of the ERα-coding region or other fragments used as fragment size controls did not have such an effect (11). This reduction might result from an effect of the ERα mRNA 3′UTR on either the stability of CAT mRNA or the translation, as in the case of interferon-β, where the 3′UTR inhibits translation (25, 26).

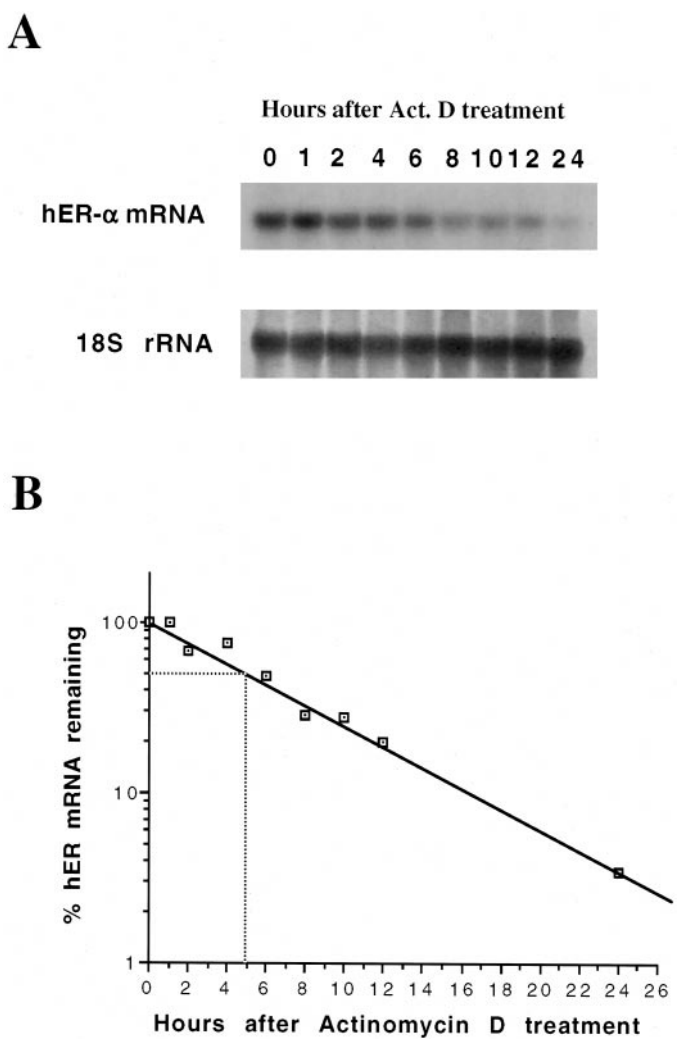

FIG. 1. Decay rate of hERα mRNA in MCF-7 cells after actinomycin D treatment. Total RNA was harvested from cells at different time points over 24 h after treatment with actinomycin D (final concentration, 0.5 μg/ml) at 0 h. A, Northern blot analysis using a probe spanning exons 1–8 of hERα mRNA (*top panel*). The 18S ribosomal RNA band visible after methylene blue staining (*bottom panel*) was used as a loading control. B, Densitometric analysis was performed on the above Northern blots, and values were plotted on a log scale against time. From this, the half-life, *i.e.* 50% of mRNA remaining after time zero, was calculated to be 5 h in the presence of actinomycin D.

To determine whether the 3′UTR of the hERα mRNA mediates rapid mRNA turnover, the decay rate of a reporter transcript containing hERα 3′UTR was measured directly in stably transfected cells using an accurate method involving a serum-inducible expression system (20, 27, 28). This method takes advantage of the transient nature of induction of the c-*fos* promoter upon serum stimulation (29) and avoids the use of artificial transcription inhibitors that can modify mRNA half-lives (18, 28). In the following experiments, the c-*fos* promoter controlled the expression of a GH chimeric gene (fGH) (20) that contained unique restriction sites in its 3′UTR region allowing the insertion of various hERα 3′UTR sequences (Fig. 2). The fGH mRNA, which contains no insert, was previously shown to have a half-life of more than 24 h (20). The vectors expressing fGH chimeric genes (pfGH) with or without hERα 3′UTR sequences were then stably transfected into HeLa cells. The half-lives of the chimeric fGH mRNAs were measured by densitometric scanning of hybridizing bands in Northern blotting experiments at various time points after serum stimulation. The probe used for this analysis was specific for the GH-coding region.

Figure 3A shows the typical results obtained from cells stably transfected with either the parental pfGH vector or pfGH plus 3.9 kb of hERα 3′UTR. In Fig. 3C, densitometric analysis of the autoradiographs was used to plot the intensity of the signals. To directly determine the half-lives, only the values corresponding to the part of the curves with a linear decay were used. As deduced from this graph, the half-life conferred upon the fGH transcript by the hERα 3′UTR was 3–4 h (Fig. 3C). No significant decay of the parental fGH transcript was detectable even 24 h after the serum stimulation. A second transcript, approximately 2 kb shorter than the normal fGH transcript, was also detected by the GH probe in the HeLa cells expressing the chimeric gene fGH+hERα 3′UTR. Hybridization analysis with probes spanning the 3′UTR of the hERα mRNA (UTR1–4 probes, see below) indicated that sequences beyond approximately the first 2 kb of the 3′UTR were not present in the shorter transcript (Fig. 3B). Its pattern of degradation paralleled that of the full transcript. Therefore, in both chimeric transcripts, a relatively short half-life was conferred by the presence of hERα 3′UTR sequences. These data confirmed the presence of a mRNA-destabilizing element in the 3′UTR of hERα mRNA.

A 1-kb subfragment of hERα 3′UTR (UTR2) retains significant ability to destabilize the fGH transcript

To delineate the region(s) in the 4.3-kb hERα 3′UTR responsible for this destabilizing activity, further fGH chimeric

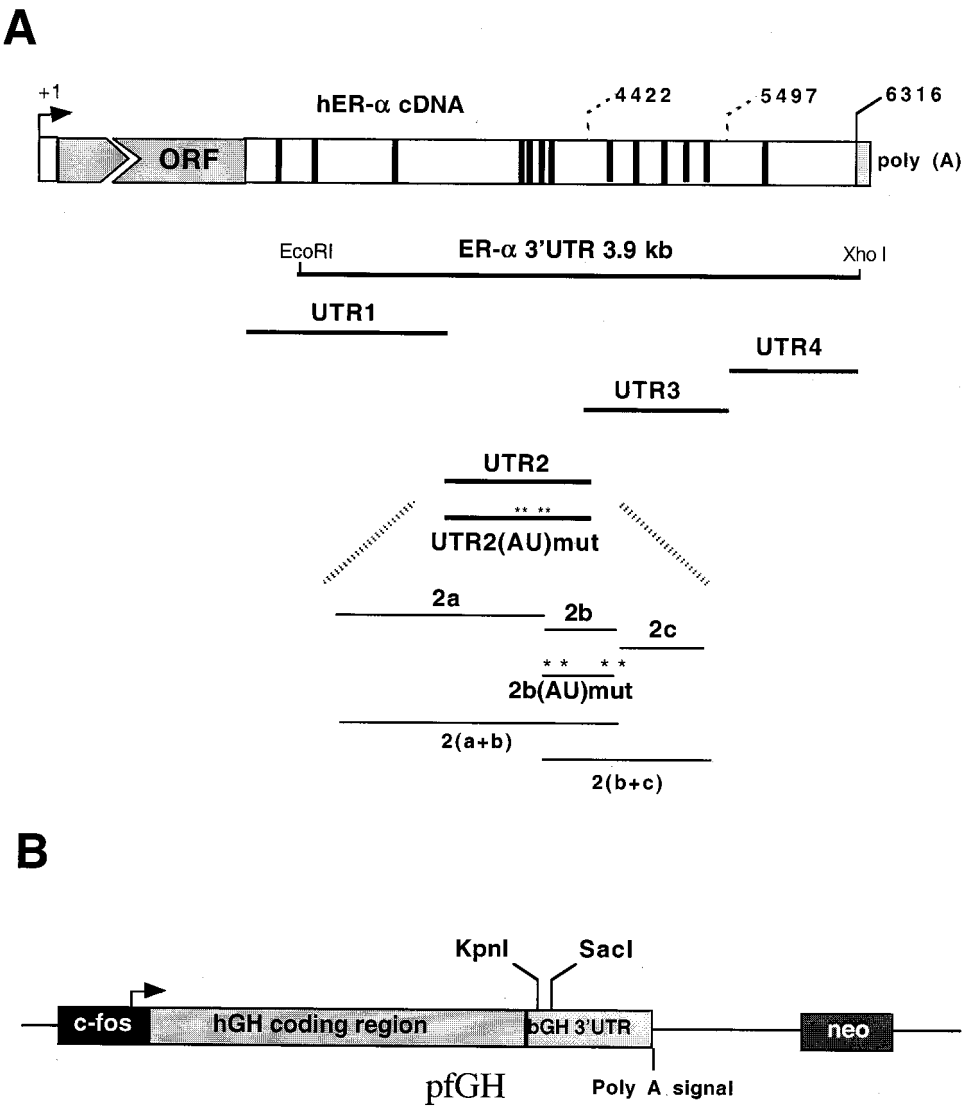

FIG. 2. Schematic representation of the 3′UTR of hERα complementary DNA and the expression vector pfGH used for stable transfections. A, Diagram of hER 3′UTR and subfragments that were inserted into the expression vector pfGH. The two potential internal poly(A) signals are shown at +4422 and +5497, and the poly(A) signal that is normally used is indicated at +6316. The positions of AUUUA motifs are shown as *thick vertical lines*. The sizes and the location of the hERα fragments relative to each other are shown on the *lower part* of A. There are the 3.8-kb *Eco*RI/*Xho*I fragment and UTR1, UTR2, UTR3, and UTR4, which span the entire 4.3-kb 3′UTR. By zooming in further, the relative locations of UTR2a-c, UTR2(a+b), and UTR2(b+c) are shown. Mutations of ATTTA to ACCCA in UTR2(AU)mut and UTR2b-(AU)mut are indicated by *asterisks*. B, The pfGH vector is shown diagrammatically. c-*fos* represents the serum inducible chicken c-*fos* promoter, followed by the human GH (hGH)-coding region and then the bovine GH (bGH) 3′UTR. The bGH 3′UTR contains a *Kpn*I/*Sac*I site, where all fragments were inserted, followed by a poly(A) signal. The neo box indicates that the neomycin resistance gene is also contained in the vector.

gene constructs were made. Thus, the entire hERα 3′UTR was subdivided into four PCR-generated fragments of approximately equivalent sizes: UTR1 (1.4 kb), UTR2 (1 kb), UTR3 (1 kb), and UTR4 (0.8 kb; Fig. 2A). The hERα 3′UTR begins at +2034, and because the *Eco*RI/*Xho*I 3.8-kb fragment, which was used in the fGH+hERα 3′UTR construct, started at +2369, the first 335 nucleotides of the 3′UTR that were not yet tested were included in UTR1. The time course for measuring decay rates of the new chimeric fGH mRNAs was carried out as described above. The approximate half-lives were as follows: 1) fGH+UTR1, 20 h; 2) fGH+UTR2, 4–5 h; 3) fGH+UTR3, 18 h; and 4) fGH+UTR4, 13 h (Fig. 4). Therefore, UTR2 was the only subfragment that retained any significant ability to destabilize the transcript, although all chimeric fGH transcripts were somewhat less stable than the fGH transcript that contained no insert. Finally, as in HeLa cells expressing the chimeric gene fGH+hERα 3′UTR, a second shorter fGH transcript was also detected in the cells stably transfected with the chimeric gene fGH+UTR2 (Fig. 4A). Size and Northern blot analyses of this RNA showed that it was similar to the short transcript observed previously for fGH+hERα 3′UTR (data not shown).

A stretch of four AUUUA motifs within UTR2 does not mediate mRNA destabilization

Sequence analysis of UTR2 revealed the presence of four AUUUA motifs in tandem (Fig. 2A). The motif AUUUA is present in the 3′UTRs of many unstable mRNAs, and evidence implicating it as a destabilizing sequence has permeated the literature. Therefore, the four AUUUA motifs within UTR2 were mutated to ACCCA, generating the construction fGH+UTR2(AU)mut (Fig. 2A). In parallel, two other chimeric genes were also made: fGH+UTR2b, which contained a UTR2 subfragment restricted to the region in which the four AUUUA motifs are located, and fGH+UTR2b(AU)mut, a mutant of fGH+UTR2b with all four AUUUA motifs changed to ACCCA (Fig. 2A). Constructs were stably integrated into HeLa cells, and the fGH transcript decay rates were studied by performing time

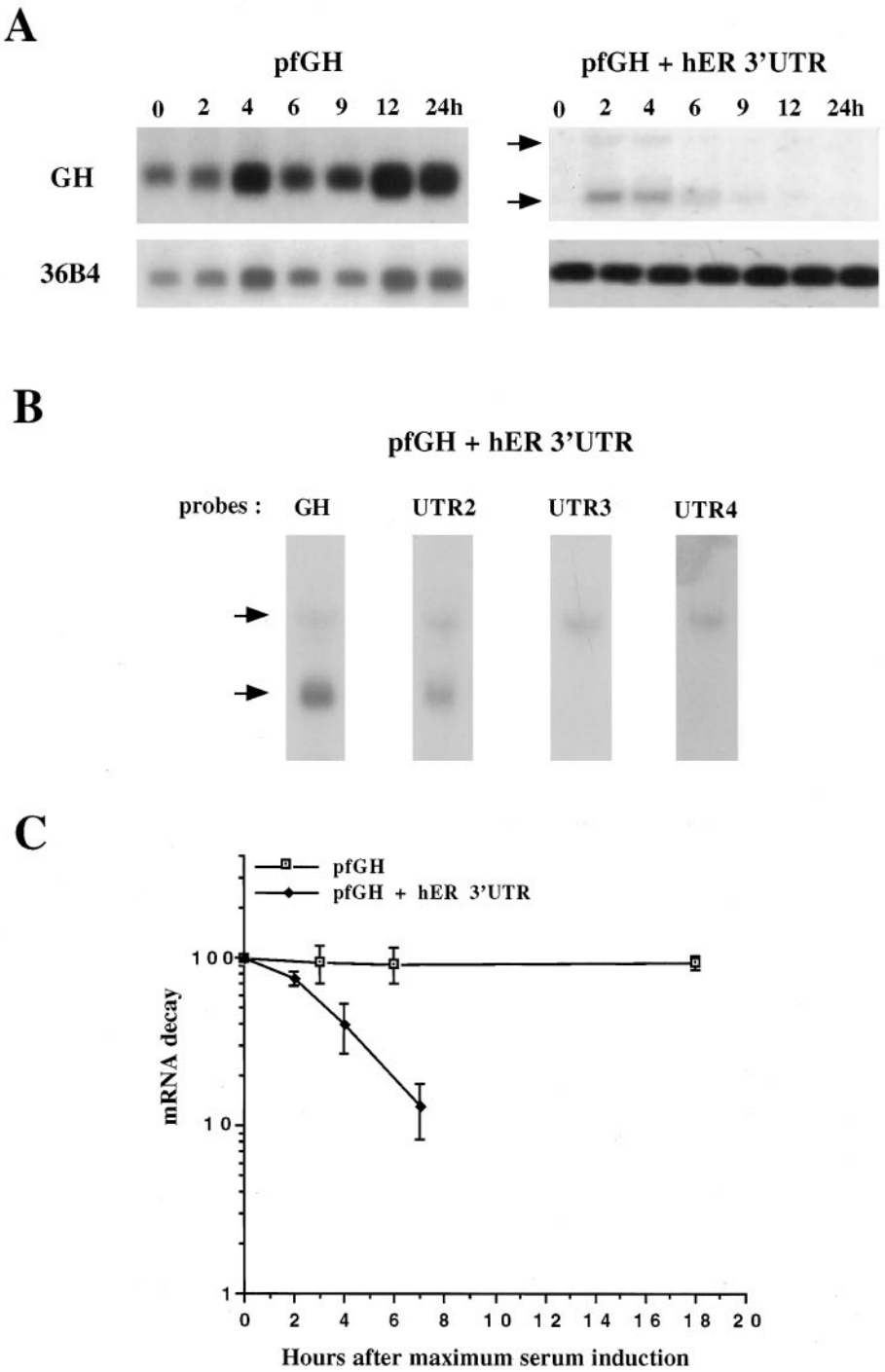

FIG. 3. Decay rate of a chimeric fGH transcript containing 3.8 kb of hERα 3′UTR. A, RNA was harvested at points from 0–24 h after serum stimulation of cells stably expressing fGH transcripts with or without the ERα 3′UTR insertion (fGH+hER 3′UTR). Northern analysis was performed using a probe for the hGH-coding region (*upper panel*). The presence of two fGH+hER 3′UTR transcripts is indicated by *arrows*. Membranes were stripped and rehybridized with a probe for 36B4, the control mRNA (*lower panel*). Representative autoradiographs are shown. B, Northern blot analysis of the two fGH+hER 3′UTR transcripts using probes spanning the 3′UTR of hERα mRNA (UTR2–4 probes) and the GH-coding region (GH; see Fig. 2A for the location of this probes). C, After densitometric analysis of the autoradiographs in A and normalization with 36B4 values, relative signal intensities after the maximum induction time point were plotted against time. To directly determine the half-lives, only the values corresponding to the part of the curves with a linear decay are shown. Each value represents the mean ± SD of three distinct experiments. In parallel, the half-lives of the chimeric fGH transcripts were determined for each experiment, and the mean ± SD between the different experiments were then calculated (fGH, >20 h; fGH+hER 3′UTR, 3.5 ± 0.5 h; $P < 0.01$ compared with fGH, by ANOVA, Fisher test).

courses as described previously. Surprisingly, the results of this experiment demonstrated that mutation of the four AUUUA motifs within UTR2 fragment did not affect the instability conferred upon the fGH reporter transcript by UTR2 (Fig. 5). The half-life of fGH+UTR2(AU)mut transcript (~3 h) was comparable to that of fGH+UTR2. Furthermore, neither the fGH transcript containing the four AUUUA motifs of UTR2, the UTR2b fragment (fGH+UTR2b $t_{1/2}$ >20 h), nor the same fragment in which the AUUUA motifs were mutated [fGH+UTR2b(AU)mut $t_{1/2}$ >20 h] caused any destabilization. These data suggested that a process other than AUUUA-mediated mRNA destabilization was responsible for the rapid mRNA turnover conferred by UTR2 sequences.

A cooperative role between different UTR2 subregion is required for the destabilizing effect

To define more precisely the region(s) in UTR2 responsible for the destabilizing activity, UTR2 was subdivided

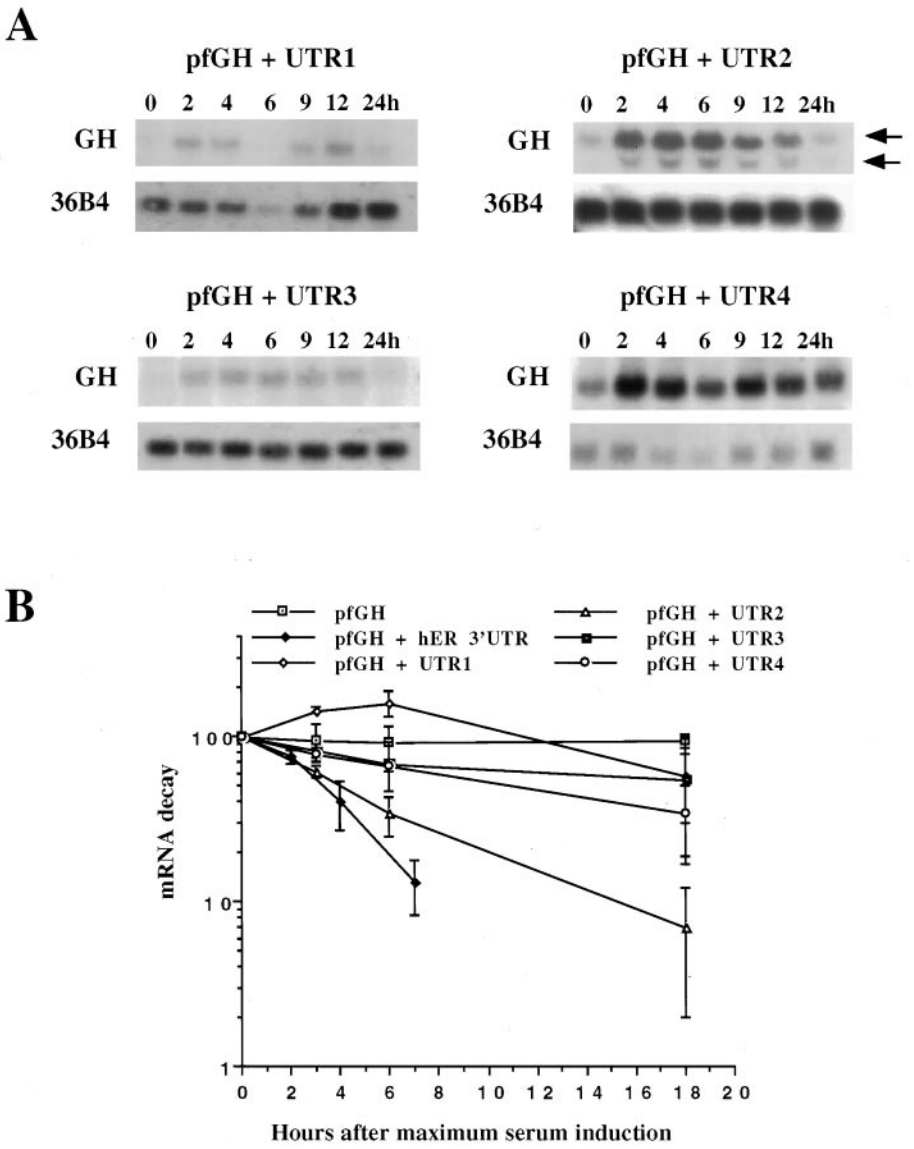

FIG. 4. Time course for chimeric fGH transcripts containing subfragments of hERα 3′UTR. A, RNA was harvested at different times after serum stimulation of cells stably transfected with pfGH vector containing the UTR1, UTR2, UTR3, or UTR4 subfragments of hERα 3′UTR (see Fig. 2A for the locations of these subfragments). Northern analysis was performed as described in Fig. 3A. The presence of two fGH+UTR2 transcripts is indicated by *arrows*. B, A graph illustrating the decay rate was drawn after densitometric analysis as described in Fig. 3B. The time-course curves for fGH and pfGH+ER 3′UTR were also included for comparison. Each value represents the mean ± SD for distinct experiments. In parallel, the half-live of the chimeric fGH transcripts was determined for each experiment, and the mean ± SD between the different experiments was then calculated [fGH, >20 h; fGH+hER 3′UTR, 3.5 ± 0.5 h; fGH+UTR1, 20 ± 4 h; fGH+UTR2, 4.5 ± 1 h ($P < 0.01$ compared with fGH, fGH+UTR1, fGH+UTR3, or fGH+UTR4, by ANOVA, Fisher test); fGH+UTR3, 18 ± 6 h; fGH+UTR4, 13 ± 2 h).

further into three smaller fragments to make constructs fGH+UTR2a–c (Fig. 2A). The constructs were then stably transfected into HeLa cells and analyzed as before. Figure 6 shows the decay rates obtained with the new fGH transcripts. The approximate half-lives for fGH+UTR2a, fGH+UTR2b, and fGH+UTR2c were 12–13 h, more than 20 h, and 20 h, respectively. Although fGH+UTR2a had the lowest stability, this messenger was much more stable than the fGH transcript with the complete UTR2 fragment. Thus, none of the UTR2a–c fragments retained the ability to destabilize the fGH transcript significantly. It appears therefore that the destabilizing activity of UTR2 was disrupted by subdividing it into the three fragments, UTR2a–c.

In many unstable mRNAs, interplay of several functionally and structurally distinct domains has been shown to be required for mRNA-destabilizing function (30–33). Such a process could also be involved in the hERα UTR2-destabilizing effect. Therefore, new chimeric genes were constructed by recombining two of the three UTR2 subfragments (UTR2a–c), fGH+UTR2(a+b) and fGH+UTR2(b+c) (Fig. 2A). The decay rates of the corresponding fGH transcripts were compared with those of fGH+UTR2 and fGH+UTR2a-c (Fig. 6). Whereas the half-life of fGH+UTR(b+c) was 20 h, the half-life of fGH+UTR2(a+b) was approximately 8–9 h, which, compared with 4 h for fGH+UTR2, indicates that UTR2(a+b) retains a major, but not total, destabilizing activity (Fig. 6). It appears likely that cooperation among the different UTR2 subfragments is required for the destabilizing effect and that the complete UTR2 fragment (+3384 to+4464) plays an essential role in defining the stability of the hERα mRNA.

Discussion

Rapid turnover of mRNA leads to low steady state levels of the mRNA for a given gene and is often used to control the concentration of the encoded protein. Such a process is

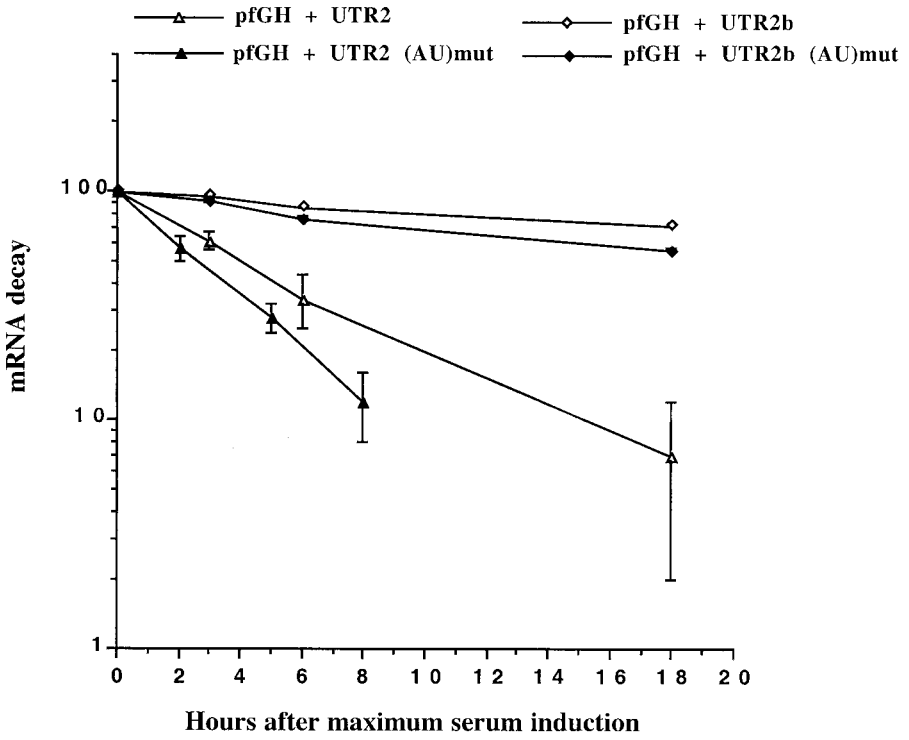

FIG. 5. A stretch of four AUUUA motifs within UTR2 does not mediate mRNA destabilization. RNA was harvested at different times after serum stimulation of cells stably expressing fGH transcripts containing UTR2, UTR2(AU)mut, or the subfragments UTR2b and UTR2b(AU)-mut (see Fig. 2A for the locations of these fragments). UTR2b corresponded to the region of UTR2 containing the four AUUUA motifs. UTR2(AU)mut and the subfragment UTR2b(AU)mut were equivalent to UTR2 and UTR2b, respectively, except that the four AUUUA motifs were mutated to ACCCA. Northern analysis was performed as described in Fig. 3A, and a graph illustrating the decay rate of fGH transcripts was drawn after densitometric analysis as described in Fig. 3B. Each value represents the mean ± SD of three distinct experiments. In parallel, the half-lives of the chimeric fGH transcripts were determined for each experiment, and the mean ± SD between the different experiments was then calculated [fGH+UTR2, 4.5 ± 1 h; fGH+UTR2(mut), 3 ± 1 h; fGH+UTR2b, >20 h; fGH+UTR2b(mut), > 20 h].

often involved in the control of expression of proteins that play a key regulatory role when a particular concentration may be critical, *e.g.* protooncogenes c-*fos* (15) and c-*myc* (16), the cytokine granulocyte-macrophage colony-stimulating factor (17), and a number of interleukins and interferons (18, 19). The ERα is an inducible transcription factor whose level has been shown to be controlled in a tissue- and development-specific manner (1, 5). Generally, estrogen target genes have different sensitivities to the loaded ER, and their transcriptional response is often rate limited by the receptor concentration in the cell (34, 35). Therefore, it is vital that the ERα level is rigidly controlled to ensure appropriate target gene expression. A relatively high mRNA turnover rate could be one mechanism, in conjunction with transcription controls, for maintaining the ERα at suitable levels.

Using the transcriptional inhibitor actinomycin D, and in agreement with a previous study (7), we showed that the endogenous hERα mRNA in MCF-7 cells could be considered unstable, with a half-life of approximately 5 h. Actinomycin D is known to cause widespread transcription inhibition in the cell and to have a severe impact on cellular physiology, which has been shown in a number of situations to prolong the life of unstable mRNAs (18, 28, 36). This may imply that hERα mRNA is subject to even higher turnover *in vivo*.

A role for 3′UTR in hERα mRNA turnover was previously suggested by preliminary results showing that the hERα 3′UTR specifically down-regulated the protein levels of a CAT reporter when present at the 3′-end of the transcript (11). This effect was observed in ER-positive cell lines (ZR-75–1) as well as ER-negative cell lines (HeLa), suggesting a ubiquitous underlying mechanism (11). To locate the region(s) of the hERα 3′UTR that was functionally involved in the destabilizing effect, the decay kinetics of a new set of chimeric transcripts (fGHs), controlled by the c-*fos* promoter and containing insertions of hERα 3′UTR and subfragments, were measured. The transiently inducible c-*fos* promoter allowed measurement of the rate of decay of newly synthesized transcripts after serum stimulation without the addition of inhibitors. The presence of the 3.8-kb fragment of hERα 3′UTR caused a reduction of the fGH reporter transcript half-life from more than 24 to 3–4 h. It should be noted that this half-life is shorter than the hERα half-life in MCF-7 cells treated with actinomycin D ($t_{1/2}$ = 5 h), a discrepancy that could be either cell type related or a result of actinomycin D prolonging the half-life (18, 28). When four hERα 3′UTR subfragments (UTR1–4) with an approximate size of 1 kb were analyzed, only UTR2 displayed significant destabilizing ability, with the half-life reduced to 4–5 h. As all fragments were of similar length, the possibility that the effect was merely size related is excluded.

The hERα 3′UTR has many AU-rich regions, and notably the UTR2 subfragment contains four AUUUA motifs and a 17-nucleotide uridylate stretch in close proximity (within 120 nucleotides) in addition to a 21-nucleotide adenylate stretch upstream. AREs serve as specific destabilizing sequences in the short-lived cytokine, protooncogene, and interferon mRNAs (19). Mutation of the AUUUA motif can disrupt these degradation pathways (33), presumably by interfering with the binding to the motif by specific proteins (29, 37). AREs have been classified into AUUUA-bearing AREs (class I and II) and those that do not contain AUUUA, but are U rich (class III). Classes I and II are further distinguished by the former having a few scattered AUUUA motifs coupled with a nearby U-rich stretch, whereas the class II AREs contain multiple reiterations of AUUU that can give rise to overlap-

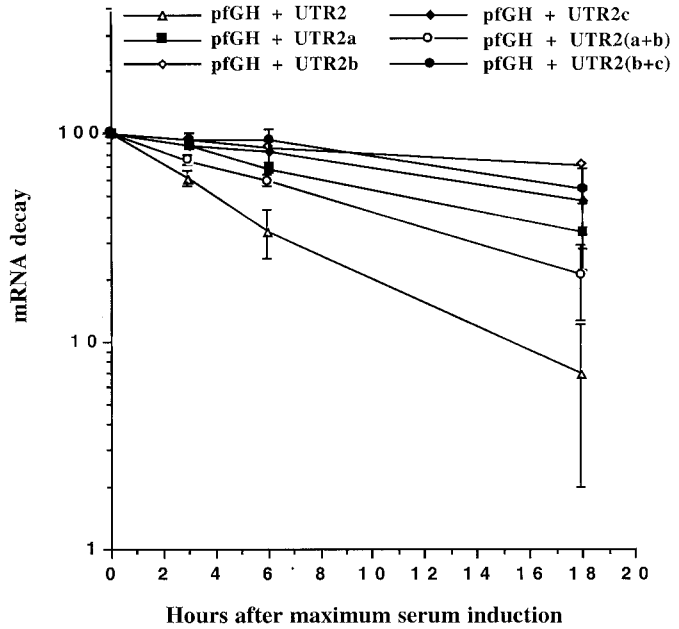

FIG. 6. A cooperative role between different UTR2 subregions is required for the destabilizing effect. RNA was harvested at points from 0–24 h after serum stimulation of cells stably transfected with pfGH vector containing the following subfragments of UTR2: UTR2a, UTR2b, UTR2c, UTR2(a+b), and UTR2(b+c) (see Fig. 2A for the locations of these subfragments). Northern analysis was performed as described in Fig. 3A. The graph illustrating the decay rate of fGH transcripts was drawn after densitometric analysis as described in Fig. 3B. The time-course curve for fGH+UTR2 is included for comparison. Each value represents the mean ± SD of three distinct experiments. In parallel, the half-lives of the chimeric fGH transcripts were determined for each experiment, and the mean ± SD between the different experiments were then calculated [fGH+UTR2, 4.5 ± 1 h; fGH+UTR2a, 12.5 ± 3 h ($P <$ 0.01 compared with fGH+UTR2, fGH+UTR2b, fGH+UTR2c, or fGH+UTR2(b+c), by ANOVA, Fisher test); fGH+UTR2b, >20 h; fGH+UTR2c, 20 ± 7 h; fGH+UTR2(a+b), 8.5 ± 2 h ($P < 0.01$ compared with fGH+UTR2b, fGH+UTR2c, or fGH+UTR2(b+c), by ANOVA, Fisher test); fGH+UTR2(b+c), 20 ± 2 h].

ping nonamers of UUAUUUAUU (36, 38). This nonamer has been proposed to be the essential minimal element in destabilization (20, 39), whereas others have proposed that the AUUUA motif is the minimal essential element (38). hERα 3′UTR does not contain the nonamer, but the AU-rich region in UTR2 is more similar to class I AREs, which are also present in other transcription factors, c-*fos* and c-*myc*. Transcripts containing class I and class II AREs are distinguished by the mechanism of degradation during polyadenylase [poly(A)] tail removal; class II AREs direct asynchronous and processive poly(A) tail digestion, and class I AREs direct synchronous and distributive deadenylation (36, 38).

The importance of the four AUUUA motifs of the hERα UTR2 fragment in the destabilizing process was tested by mutating them to ACCCA motifs [UTR2(AU)mut]. However, no obvious difference in fGH+UTR2 mRNA decay was observed regardless of whether the motifs were mutated. This result indicates that the presence of these four AUUUA motifs was not the main source of destabilization. This finding is not unprecedented, because others have found that AUUUAs were dispensable for rapid degradation of the mouse c-*myc* RNA (40, 41). In fact, a study showed that an AUUUA mutation in c-*myc* does not affect mRNA stability, but, rather, influences the subcellular localization of the transcript (42). In addition, non-AUUUA, but U-rich, elements can confer degradation, as exemplified by class III AREs.

The destabilizing activity of UTR2 was disrupted by subdividing it further into three smaller fragments, UTR2a–c. In view of this result, it was speculated that a sequence element had been inadvertently disrupted by fragmentation of UTR2. Further investigation showed that recombining UTR2a and -b fragments (UTR2a+b) partially restored the destabilizing effect, whereas recombining UTR2b and -c was ineffective. That implies that sequences from both UTR2a and -b are required for the destabilizing effect. Nevertheless, the fact that the UTR2a+b subfragment did not destabilize as strongly as UTR2 suggests the presence of other element(s) elsewhere in the UTR2, which is required for optimal degradation. Several mRNAs subject to rapid turnover contain more than one sequence element required for destabilization (30, 31), with different domains in the transcript being responsible for separate steps in the degradation pathways (32, 33).

Another mechanism to direct destabilization is through particular secondary structures adopted by the RNA. An example of this is the 3′ stem-loop structure of histone mRNA that serves as a signal for degradation (43). Also, the insulin-like growth factor II gene contains a 4-kb long 3′UTR where two domains that are critical for mRNA degradation are separated by 2 kb, but are capable of interacting via secondary structure. The stem structure and the primary sequence of this complex element are responsible for directing a site-specific endonucleolytic cleavage, which leads to rapid degradation of the insulin-like growth factor II mRNA (44). Such processes could be also involved in the hERα 3′UTR-destabilizing effect. Indeed, preliminary S1 nuclease and primer extension experiments on *in vivo* or *in vitro* transcribed mRNA containing hERα UTR2 sequences suggested the existence of a relatively stable secondary structure(s) within the UTR2 region (data not shown). The loss of such a secondary structure(s) when UTR2 was fragmented could therefore account for the disappearance of destabilizing ability. Further investigations are obviously required to test this hypothesis.

Finally, it should be noted that a second shorter transcript was also detected by the GH probe in the HeLa cells expressing both the chimeric genes fGH+hER 3′UTR and fGH+UTR2, but not fGH+UTR1, -3, or -4 or UTR2 subfragments (a, b, c, a+b, and b+c). Two mechanisms may explain this result. A potential internal poly(A) signal located in the hERα UTR2 at position +4442 may be functional in addition to that of the fGH 3′UTR that is normally used by the fGH chimeric genes. However, in this case, a second shorter transcript should have been observed for the chimeric genes fGH+UTR2c and fGH+UTR2(b+c). The alternative explanation is that an endonucleolytic cleavage occurs in the UTR2 region, thereby accounting for the shorter transcript detected by Northern blot. Indeed, the second shorter transcript is only detected with fGH mRNAs presenting a short half-life (fGH+hER 3′UTR and fGH+UTR2), which may suggest a correlation between the presence of this second transcript and the mechanism that directs mRNA destabilization conferred by UTR2 sequences. The fact that fGH+UTR2(a+b) retains a partial destabilizing activity, whereas no second shorter transcript is detected may also indicate that the hERα 3′UTR

degradation pathway requires separate steps with more than one sequence element involved in the process. As the origin of the second transcripts could be linked to the degradation pathway of hERα transcript, future studies are obviously needed to further characterize the origin of the shorter transcripts and, in turn, the mechanism leading to hERα mRNA instability and to identify the factors involved in this process.

In summary, this present study refines the characterization of the role of the 3′UTR of hERα mRNA. It shows the existence of another level in the control of expression of the ligand-activated transcription factor hER in addition to transcriptional regulation. Given the general similarities in the structure and function of members of the steroid hormone receptor gene family, it is predicted that elements that influence the stability of mRNAs of other steroid hormone receptors should also be found in their 3′UTR.

Acknowledgments

We thank Dr. Greg Goodall for providing the pfGH plasmid, Dr. Pierre Chambon for the 36B4 plasmid, and Dr. M. Keaveney for other materials.

References

1. **Auchus RJ, Fuqua SA** 1994 Hormone-nuclear receptor interactions in health and disease. The œstrogen receptor. Bailliere's Clin Endocrinol Metab 8:433–449
2. **George FW, Wilson JD** 1988 Sex determination and sex differentiation. In: Knobil E, Neil JD, Ewing LL, Greenwald GS, Market CL, Pfaff DW (eds) The Physiology of Reproduction: Sex Determination and Sex Differentiation. Raven Press, New York, pp 3–26
3. **Miesfeld R, Rusconi S, Godowski PJ, Maler BA, Okret S, Wilkstrom AC, Gustafsson JA, Yamamoto K** 1986 Genetic complementation of a glucocorticoid receptor deficiency by expression of a cloned receptor cDNA. Cell 46:389–399
4. **Henderson BE, Ross R, Bernstein L** 1988 Estrogens as a cause of human cancer: the Richard and Hinda Rosenthal Foundation award lecture. Cancer Res 48:246–253
5. **Flouriot G, Griffin C, Kenealy MR, Sonntag-Buck V, Gannon F** 1998 Differentially expressed isoforms of the human estrogen receptor-α gene are generated by alternative splicing and promoter usage. Mol Endocrinol 12:1939–1954
6. **Read LD, Green GL, Katzenellenbogen BS** 1989 Regulation of estrogen receptor messenger ribonucleic acid and protein levels in human breast cancer cell lines by sex steroid hormones, their antagonists and growth factors. Mol Endocrinol 3:295–304
7. **Saceda M, Knabbe C, Dickson RB, Lippman ME, Bronzert D, Lindsey R, Gottardis MM, Martin MB** 1991 Post-transcriptional destabilisation of estrogen receptor mRNA in MCF-7 cells by 12-*O*-tetradecanoylphorbol-13-acetate. J Biol Chem 266:17809–17814
8. **Saceda M, Lippman ME, Chambon P, Lindsey RL, Ponglikitmongkol M, Puente M, Martin MB** 1988 Regulation of the estrogen receptor in MCF-7 cells by estradiol. Mol Endocrinol 2:1157–1162
9. **Saceda M, Lippman ME, Lindsey RK, Puente M, Martin MB** 1989 Role of estrogen receptor-dependant mechanism in the regulation of estrogen receptor mRNA in MCF-7 cells. Mol Endocrinol 3:1782–1789
10. **Green S, Walter P, Kumar V, Krust A, Bornert JM, Argos P, Chambon P** 1986 Human oestrogen receptor cDNA: sequence, expression and homology to v-*erb*-A. Nature 320:134–139
11. **Keaveney M, Parker MG, Gannon F** 1993 Identification of a functional role for the 3′ region of the human oestrogen receptor gene. J Mol Endocrinol 10:143–152
12. **Koike S, Sakai M, Muramatsu M** 1987 Molecular cloning and characterisation of rat estrogen receptor cDNA. Nucleic Acids Res 15:2499–2513
13. **White R, Lees JA, Needham M, Parker MG** 1987 Structural organisation and expression of the mouse estrogen receptor gene. Mol Endocrinol 1:735–744
14. **Jacobs EC, Arnold AP, Campagnoni AT** 1996 Zebra finch estrogen receptor cDNA: cloning and mRNA expression. J Steroid Biochem Mol Biol 59:135–145
15. **Wilson T, Treisman R** 1988 Removal of poly(A) and consequent degradation of c-fos mRNA facilitated by 3′ AU-rich sequences. Nature 336:396–399
16. **Jones TR, Cole MD** 1987 Rapid cytoplasmic turnover of c-myc mRNA: requirement of 3′ untranslated sequences. Mol Cell Biol 7:4513–4521
17. **Shaw G, Kamen R** 1986 A conserved AU sequence from the 3′ untranslated region of GM-CSF mRNA mediates selective mRNA degradation. Cell 46:659–667
18. **Whittlemore LA, Maniatis T** 1990 Postinduction turnoff of β-interferon gene expression. Mol Cell Biol 10:1329–1337
19. **Greenberg ME, Belasco JG** 1993 Control of the decay of labile protooncogenes and cytokine mRNAs. In: Belasco JG, Brawerman G (eds) Control of Messenger RNA Stability: Control of the Decay of Labile Protooncogenes and Cytokine mRNAs. Academic Press, San Diego, pp 199–218
20. **Lagnado CA, Brown CY, Goodall GJ** 1994 AUUUA is not sufficient to promote poly(A) shortening and degradation of an mRNA: the functional sequence within AU-rich elements may be UUAUUUA(U/A)(U/A). Mol Cell Biol 14:7984–7995
21. **Keaveney M, Neilan J, Gannon F** 1989 An analysis by restriction enzymes of the genomic structure of the 3′ untranslated region of the human oestrogen receptor gene. Biochim Biophys Acta 1007:289–294
22. **Masiakowski P, Breathnach J, Bloch J, Gannon F, Krust A, Chambon P** 1982 Cloning of cDNA sequences of hormone-regulated genes from the MCF-7 human breast cancer cell line. Nucleic Acids Res 10:7895–7903
23. **Ausubel FM, Brent R, Kingston RE, Moore, DD, Smith JA, Seidman JG, Struhl K** 1987 Current Protocols in Molecular Biology. Greene and Wiley Interscience, New York
24. **Auffray C, Rougeon F** 1980 Purification of mouse immunoglobulin heavy-chain messenger RNAs from total myeloma tumor RNA. Eur J Biochem 107:306–314
25. **Grafi G, Sela I, Galili G** 1993 Translational regulation of human β interferon mRNA: association of the 3′AU-rich sequence with the poly (A) tail reduces translational efficiency in vitro. Mol Cell Biol 13:3487–3493
26. **Kruys V, Wathelet M, Poupart P, Contreras R, Fiers W, Content J, Huez G** 1987 The 3′untranslated region of the human interferon-β mRNA has an inhibitory effect on translation. Proc Natl Acad Sci USA 84:6030–6034
27. **Ahern SM, Miyati T, Sadler JE** 1993 Regulation of human tissue factor expression by mRNA turnover. J Biol Chem 268:2154–2159
28. **Shyu AB, Greenberg M, Belasco J** 1989 Two distinct destabilising elements in the c-fos message trigger deadenylation as a first step in rapid mRNA decay. Genes Dev 3:60–72
29. **Treisman R** 1985 Transient accumulation of c-fos RNA following serum stimulation requires a conserved 5′ element and c-fos 3′ sequences. Cell 42:889–902
30. **Kabnick KS, Housman DE** 1988 Determinants that contribute to cytoplasmic stability of human c-fos and β-globin mRNAs are located at several sites in each mRNA. Mol Cell Biol 8:3244–3250
31. **Wisdom R, Lee W** 1991 The protein coding region of c-myc mRNA contains a sequence that specifies rapid turnover and induction by protein synthesis inhibitors. Genes Dev 5:232–243
32. **Chen CYA, Chen TM, Shyu AB** 1994 Interplay of two funtionally and structurally distinct domains of the c-fos AU-rich element specifies its mRNA-destabilising function. Mol Cell Biol 14:416–426
33. **Shyu AB, Belasco J, Greenberg M** 1991 Two distinct destabilising elements in the c-fos message trigger deadenylation as a first step in rapid mRNA decay. Gene Dev 5:221–231
34. **Barton MC, Shapiro DJ** 1988 Transient administration of estradiol 17-β establishes an autoregulatory loop permanently inducing estrogen receptor mRNA. Proc Natl Acad Sci USA 85:7119–7123
35. **Flouriot G, Pakdel F, Ducouret B, Le Drean Y, Valotaire Y** 1997 Differential regulation of two genes implicated in fish reproduction: vitellogenin and estrogen receptor genes. Mol Reprod Dev 48:317–323
36. **Chen CYA, Xu N, Shyu AB** 1995 mRNA decay mediated by two distinct AU-rich elements from c-fos and granulocyte-macrophage colony stimulating factor transcripts: different de-adenylation kinetics and uncoupling from translation. Mol Cell Biol 15:5777–5788
37. **Malter JS** 1989 Identification of an AUUUA-specific messenger RNA binding protein. Science 246:664–666
38. **Xu N, Chen CYA, Shyu AB** 1997 Modulation of the fate of cytoplasmic mRNA by AU-rich elements, key sequence features controlling mRNA deadenylation and decay. Mol Cell Biol 17:4611–4621
39. **Zubiaga AM, Belasco JG, Greenberg ME** 1995 The nonamer UUAUUUAUU is the key AU-rich sequence motif that mediates mRNA degradation. Mol Cell Biol 15:2219–2230
40. **Bonnieu A, Roux P, Marty L, Jeanteur P, Piechaczyk M** 1990 AUUUA motifs are dispensable for rapid degradation of the mouse c-myc RNA. Oncogene 5:1585–1588
41. **Laird-Offringa I, Elfferichand P, van der Eb A** 1991 Rapid c-myc mRNA degradation does not require (A+U)-rich sequences or complete translation of the mRNA. Nucleic Acids Res 19:2387–2394
42. **Veyrune JL, Campbell GP, Wiseman J, Blanchard JM, Hesketh JE** 1996 A localisation signal in the 3′untranslated region of c-myc mRNA targets c-myc mRNA and β-globin reporter sequences to the perinuclear cytoplasm and cytoskeletal-bound polysomes. J Cell Sci 109:1185–1194
43. **Vasserot AP, Schaufele FJ, Birnstiel ML** 1989 Conserved terminal hairpin sequence of histone mRNA precursors are not involved in duplex formation with the U7 RNA but act as a target site for a distinct processing factor. Proc Natl Acad Sci USA 86:4345–4349
44. **Scheper W, Meinsma D, Holthuizen PE, Sussenbach JS** 1995 Long-range RNA interaction of two sequence elements required for endonucleolytic cleavage of human insulin-like growth factor II mRNAs. Mol Cell Biol 15:235–245